Hybrid Modeling of Curved Fault Radiation in a 3D Heterogeneous Medium

Kim B. Olsen[(1)], Eiichi Fukuyama[(2)], Hideo Aochi[(3)] and Raul Madariaga[(3)],

(1) Institute for Crustal Studies, University of California, Santa Barbara, USA (e-mail: kbolsen@crustal.ucsb.edu; phone: 805 893 7394; fax: 805 893 8649). (2) Eiichi Fukuyama, National Institute for Earth Science and Disaster Prevention, Tsukuba, 305-0006, Japan (email: fuku@bosai.go.jp; phone: (81)2-9851-1611; fax: (81)2-9854-0629). (3) Laboratoire de Géologie, Ecole Normale Supérieure, 24 rue Lhomond, 75231 Paris Cedex 05, France (e-mail: madariag@dorrite.ens.fr; phone: +33-1-44322216; fax: +33-1-44322200).

Abstract

We are in the process of the development of a hybrid method for flexible and efficient modeling of dynamic rupture propagation and its radiation in a heterogeneous three-dimensional medium. The dynamic rupture propagation is computed using the boundary integral equation (BIE) method. The computation of radiated waves outside the fault is carried out by an efficient fourth-order staggered-grid finite-difference (FD) method. The hybrid method enables dynamic modeling of rupture propagation on curved or multi-segmented faults in laterally and vertically heterogeneous earth models with an accurate free-surface. In addition to the model of dynamic rupture on a single fault, the hybrid method can be used to model the statistics of recurrent ruptures on multiple, arbitrarily-shaped fault systems. Finally, the method may be used to improve the accuracy of kinematic source implementation on extended faults.

Introduction

The conventional earthquake rupture models have been restricted to planar fault geometries due to the extremely complex formulation of the dynamics (e.g., Madariaga et al., 1998[1]. Moreover, these studies have traditionally been limited to studies of the nature of the dynamic rupture itself on the fault, neglecting the radiation of waves away from the fault. An exception is the computation of dynamic radiation for the 1992 Landers earthquake and its comparison to strong motion data (Olsen et al., 1997[2]; Peyrat et al., 2000[3]), which, however, still was limited to planar fault geometries. For FD grids, the computation of dynamic conditions and radiation for dipping, planar faults can easily be carried out (e.g., Nielsen and Olsen, 2000[4]), while such efforts for curved faults are excessively complicated. Other modeling methods, in particular the boundary integral element (BIE) method, is capable of including the dynamic conditions for curved faults (e.g., Fukuyama and Madariaga, 1998[5]). Recently, Aochi et al. (Aochi et al., 1999[6]; 2000[7]) pointed out the importance of including curved fault geometries, because the stress field may be affected by the dynamic rupture on complex fault geometries. For example, Aochi et al. found that rupture propagation is de-cellerated or arrested for some inclined angle of a bending fault under tri-axial compression. Also, they found that rupture propagation on branching faults depended strongly on the angle of the branch. The latter result may have affected the rupture propagation on the 1992 Landers earthquake, which occurred on three different segments, also investigated by Aochi and Fukuyama (2000)[8].

While BIE methods can handle arbitrarily complex friction laws on the fault, the computation of radiated waves away from the fault is very expensive. Here, FD methods have excelled due to their computational efficiency and flexibility to define arbitrarily heterogeneous crustal models, allowing for large-scale wave propagation simulations (e.g., Olsen et al., 1995[9]).

Our aim here is to develop a method that captures the desirable features of the different approaches: the flexibility of dynamic rupture propagation on non-planar or multi-segmented fault geometries from the BIE method, and the efficient wave propagation of elastic waves in heterogeneous media using the FD method. We propose to develop a hybrid method for flexible and efficient modeling of dynamic rupture propagation and its radiation in a heterogeneous three-dimensional medium. The free-surface, which has been implemented in BIE methods only with limited accuracy, is included in the hybrid method with the same high accuracy as obtained in the FD grid.

Interfacing BIE and FD Schemes

The main idea of the hybrid method is to confine one or several regions containing the dynamic fault propagation solved by BIEM within the larger FD grid and develop the proper interaction between the rupture and its radiation. The BIEM was described in Fukuyama and Madariaga (1998[5]). While the wavefield parameters (e.g., stresses and displacement/velocity) are located at the same positions in the 3D grids for the BIEM, we use a staggered grid for the finite differences to solve the 3-D elastic equations of motion (Olsen, 1994[10]). We use the absorbing boundary conditions by Clayton and Engquist (1977[11]), and the sides of the computational model are padded with homogeneous regions of attenuative material to further limit reflections from the boundaries of the grid (Cerjan et al., 1985[12]).

An earlier study (Olsen et al., 1995[9]) showed how to insert a kinematic source (point as well as extended fault) in the finite-difference grid by adding

$$-\Delta t \dot{M}_{ij}(t)/V \tag{1}$$

to $S_{ij}(t)$, where $\dot{M}_{ij}(t)$ is the ijth component of the moment rate tensor for the earthquake, V $= dx^3$ is the cell volume, and $S_{ij}(t)$ is the ij-th component of the stress tensor on the fault at time t. We extend this method to a procedure for incorporating the BIEM dynamic rupture along an arbitrary fault plane into the FD grid. Figure 1 shows how the BIEM slip rate at an arbitrary point (x, y, z) can be distributed to the closest eight FD grid points using bilinear interpolation. Using the weights

$$t = (x - x(i,j,k)/(x(i+1,j,k) - x(i,j,k)) \tag{2}$$

$$u = (y - y(i,j,k)/(y(i,j+1,k) - y(i,j,k)) \tag{3}$$

$$v = (z - z(i,j,k)/(z(i,j,k+1) - z(i,j,k)) \tag{4}$$

we compute the values at the FD grid points as

$$(1-t)\cdot(1-u)\cdot(1-v) \quad at \quad (x,y,z) \tag{5}$$

$$t\cdot(1-u)\cdot(1-v) \quad at \quad (x+1,y,z) \tag{6}$$

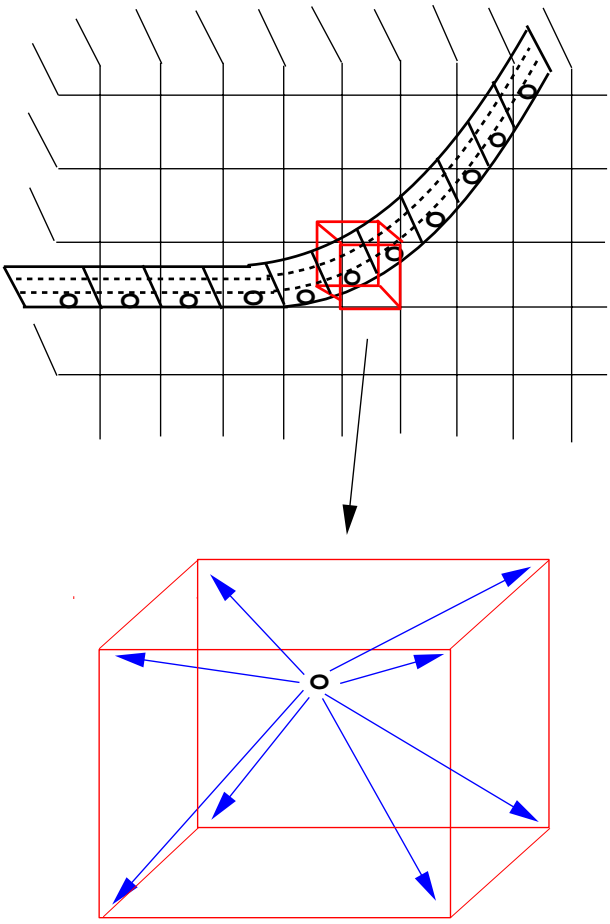

Figure 1: Distribution of the moment as an extrapolation from the center of the BIEM element to the eight surrounding FD grid points.

$$t \cdot u \cdot (1-v) \quad at \quad (x+1, y+1, z) \tag{7}$$

$$(1-t) \cdot u \cdot (1-v) \quad at \quad (x, y+1, z) \tag{8}$$

$$(1-t) \cdot (1-u) \cdot v \quad at \quad (x, y, z+1) \tag{9}$$

$$t \cdot (1-u) \cdot v \quad at \quad (x+1, y, z+1) \tag{10}$$

$$t \cdot u \cdot v \quad at \quad (x+1, y+1, z+1) \tag{11}$$

$$(1-t) \cdot u \cdot v \quad at \quad (x, y+1, z+1) \tag{12}$$

Preliminary Numerical Results for a Single Curved Fault

We tested the procedure described above for a curved fault (see Figure 2), taken from Aochi et al. (2000[7]). Figure 3 shows the horizontal and vertical particle velocity in a plane perpendicular to the fault, along its central axis. The final slip distribution is shown in Figure 2. Figure 4 shows the velocity seismograms along the plane where the snapshots in

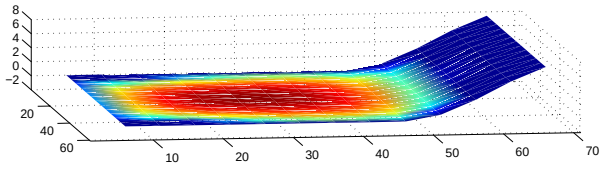

Figure 2: Curved fault geometry with final slip distribution.

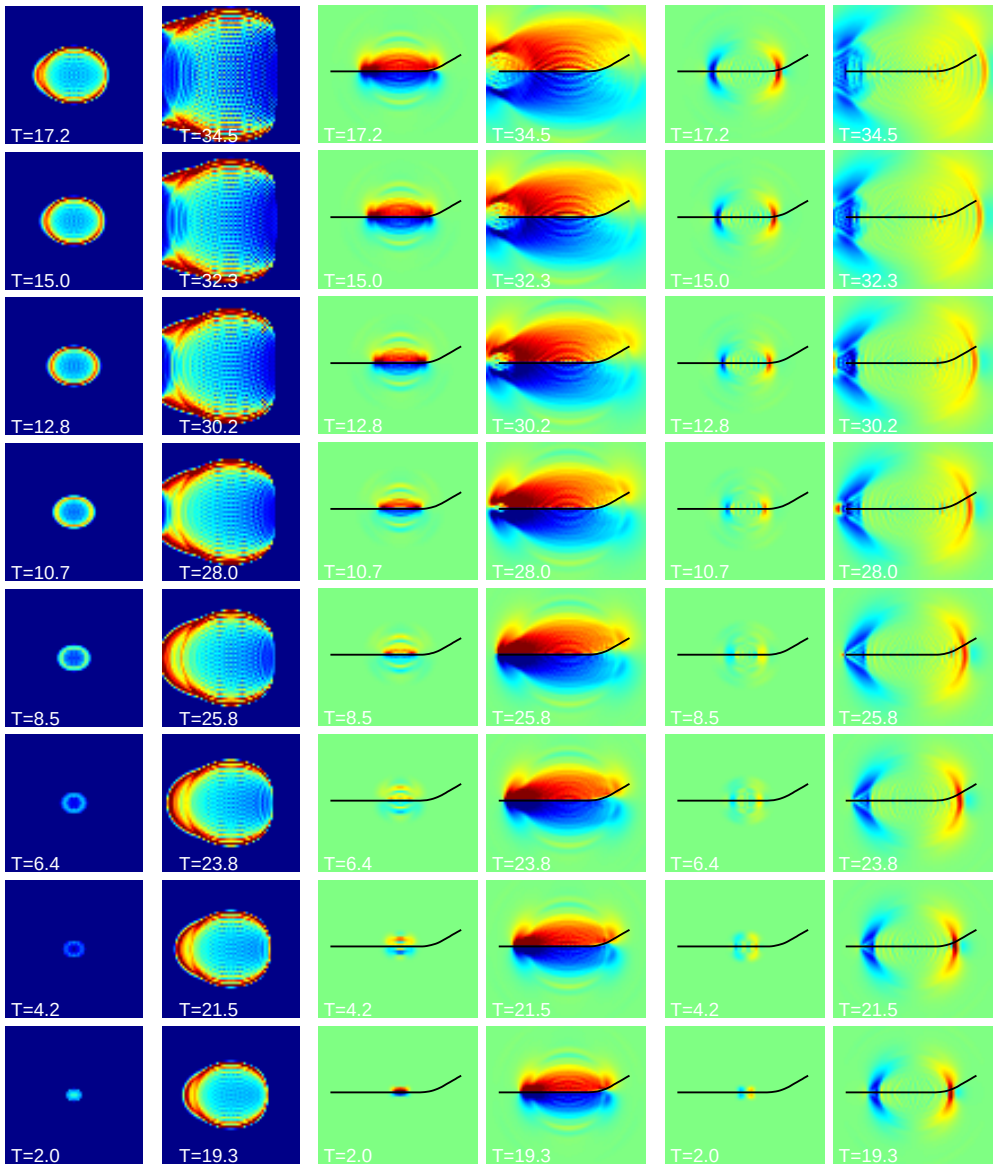

Figure 3: Radiation on the horizontal (middle) and vertical (right) components from the curved fault on a plane perpendicular to the fault. Solid line in each panel corresponds to the fault trace. The slip velocity distribution on the fault is also shown (left).

Figure 3 were taken. At time T=15, the rupture fronts have reached the curved part of the fault. At time T=20, the effect of the curvature of the fault starts to appear, i.e., note the asymmetry of the wavefield. While limited because the dominant slip occurs on the planar part of the fault, the asymmetry is also apparent in the seismograms in Figure 3. This is particularly the case for the static offset of the fault parallel motion.

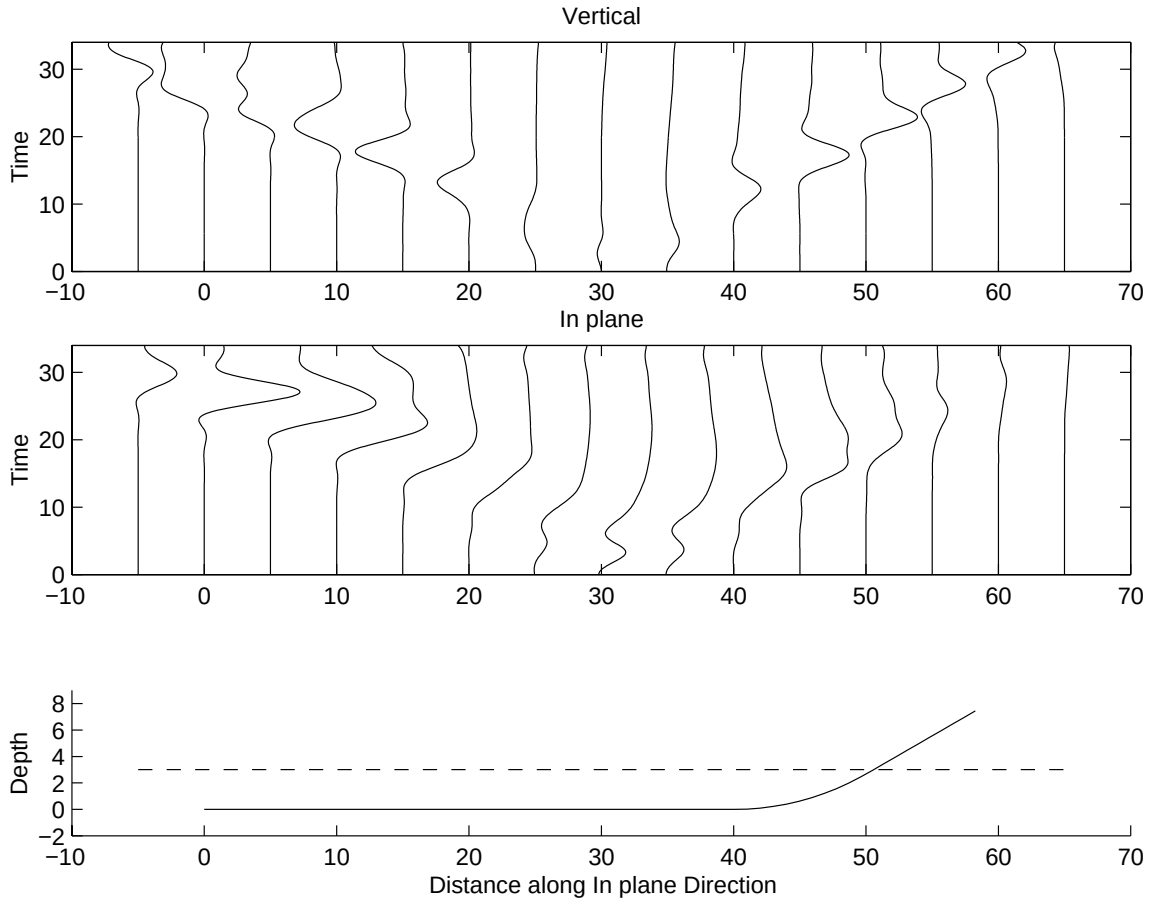

Figure 4: Radiation from the curved fault, along the line intersecting the fault along its axis (see lower plot).

Future Work

In a heterogeneous medium, or in the presence of a free surface or interference between several faults, the stresses on the faults need to be updated in order to account for the proper interaction. We plan to implement this feedback by adding the stresses from the FD radiation onto the BIEM fault plane, using a bi-linear interpolation, similar to the procedure described above.

We will investigate ways to validate the dynamic radiation from the hybrid method to that for the FD method for planar and curved faults in full space and halfspace models. We will also apply the method to the 1992 Landers and 1999 Chi-Chi earthquakes, assess the effects of fault segmentation and curvature on dynamic rupture propagation and its dynamic radiation, and compare radiated waves to strong motion data. We believe that the studies of radiation from non-planar fault geometries are extremely important to understand the near-field behavior of strong ground motion.

Acknowledgments

The computations in this study were partly carried out on the SUN Enterprise at MRL/ICS, UCSB with support from the Southern California Earthquake Center (SCEC), USC 572726 through the NSF cooperative agreement EAR-8920136. R. Madariaga's work was supported by the Environment Program of the European Community under project SGME.

References

[1] Madariaga, R., Olsen, K.B. and Archuleta, R., 1998, *Modeling dynamic rupture in a 3D earthquake fault model,* Bull. Seis. Soc. Am. **88**, 1182-1197.

[2] Olsen, K., Madariaga, R., and Archuleta, R., 1997, *Three dimensional dynamic simulation of the 1992 Landers earthquake,* Science **278**, 834-838.

[3] Peyrat, S., K.B. Olsen, R. Madariaga, 2000, *Dynamic modeling of the Landers, California, earthquake,* Jour. Geophys. Res., submitted.

[4] Nielsen, S.B., and Olsen, K.B., 2000, *Three-dimensional dynamic rupture models of the 1994 Northridge, California, earthquake,* PAGEOPH, accepted for publication.

[5] Fukuyama, E., and Madariaga, R., 1998, *Rupture dynamics of a planar fault in a 3D Elastic medium: Rate- and slip- weakening friction,* Bull. Seismol. Soc. Am. **88**, 1-17.

[6] Aochi, H., Fukuyama, E., and Matsu'ura, M., 1999, *Dynamics of rupture propagation on 3D complex faults,* EOS Trans. AGU **80**, F755.

[7] Aochi, H., Fukuyama, E., and Matsu'ura, M., 2000, *Spontaneous rupture propagation on a non-planar fault in 3D elastic medium,* PAGEOPH, accepted for publication.

[8] Aochi, H., and Fukuyama, E., 2000, *3-D non-planar simulation of the 1992 Landers earthquake,* (in preparation).

[9] Olsen, K., Archuleta, R., and Archuleta, R., 1995, *Three dimensional simulation of a M 7.75 earthquake on the San Andreas Fault,* Science **270**, 1628-1632.

[10] Olsen, K., 1994, *Simulation of three-dimensional wave propagation in the Salt Lake Basin,* Ph.D. Thesis, University of Utah, Salt Lake City, Utah, 157 p.

[11] Clayton, R., and Engquist, B., 1977, *Absorbing boundary conditions for acoustic and elastic wave equations,* Bull. Seism. Soc. Am. **71**, 1529-1540.

[12] Cerjan, C., Kosloff, D. Kosloff, R. and Reshef, M., 1985, *A nonreflecting boundary condition for discrete acoustic and elastic wave equations,* Geophysics **50**, 705-708.